An innovative Hardware-In-the-Loop rig for linear Power-Take-Off testing

G. Alessandri, F. Gallorini, L. Castellini, D. Montoya, E. F. Alves and E. Tedeschi

Abstract— **This paper describes the activities related to the design, manufacturing and commissioning of an innovative Hardware-In-the-Loop test rig for linear Power Take-Off testing within the Horizon 2020 IMAGINE project. The rig is characterised by a fully coupled architecture in which three electro-mechanical units integrating a ballscrew and an electrical machine can actuate on a linear axis, either as motor or generator. A preliminary mechanical design of the test rig was carried out by identifying the most demanding conditions. The electrical and mechanical designs were assessed through a de-risking simulation of the overall test rig set-up, considering faults between the motors and respective power converters. The resulting rig setup includes a structure that embeds the three units, an electrical control panel and a control system. The use of electro-mechanical units increases the flexibility of the setup and simplifies the test of extreme conditions such as maximum output power or actuation force. Moreover, it allows reusing the power produced by the generating devices, thus reducing operational costs of the tests. The control system integrates a real-time hardware-in-the-loop simulation platform, a supervisory control and data acquisition systems. Those offer not only the possibility of easily tuning parameters but also testing new control strategies, operational situations, and failures of a power-take-off system in very realistic conditions.**

Keywords— **Hardware-In-the-Loop testing; Power Take-Off; test rig; electro-mechanical system; numerical modelling, Wave Energy Converter.**

I. Introduction

WAVE Energy Converters (WECs) development is a complex topic due to multiple aspects being considered: variability of the input loads, harsh marine environment, high installation and maintenance costs. Those are only some of the aspects that prevented wave energy to reach a technical and commercial maturity comparable to other renewable energy technologies [1]. Among the subsystems in a WEC, Power Take-Offs (PTOs) are of primary importance: their role in converting the input mechanical energy to output electrical energy and aspects such as reliability, survivability, controllability and maintainability have an impact on the energy yield of the overall device [1]. In addition, PTOs account for the 22% of the costs in a typical wave energy project [2]. Integration of PTOs with other key subsystems should be pursued from the early design phase of a WEC, both with real and simulated tests.

Simulated environments are widely adopted in the aerospace, automotive, power generation, industrial, robotics and medical sectors. The Hardware-In-the-Loop (HIL) testing scheme is considered as a state-of-the-art tool to bridge the gap between the laboratory and operational environment. In the wave energy sector, HIL has already been used for testing PTOs, as described in [3], [4], [5] and [6].

The present work adds a new contribution to these previous efforts by describing the activities related to the design, manufacturing, and commissioning of an innovative HIL test rig for linear PTO testing.

II. Background

The EU-funded IMAGINE project aims at designing, manufacturing, and rig-testing a linear generator for wave energy applications. The final goal of the project is to prove the generator:

- Efficiency, with a target range of 70-85%;
- Reliability, with a target Mean Time Between Failures (MTBF) of 20 years;
- Affordability, with a target CAPEX reduction by over 50% compared to state-of-the-art PTOs.

IMAGINE brings together cross-functional ocean energy competences from six partners across Europe: UMBRAGROUP spa (PTO manufacturer), VGA (test rig manufacturers), Norwegian University of Science and Technology (NTNU, control system experts), K2 Management (marine renewables engineering consultants), the University of Edinburgh (academics with knowledge in techno-economic analyses) and Bureau Veritas (certification body).

Paper ID number: 2323.

The IMAGINE project has received funding from the European Union's Horizon 2020 research and innovation programme under grant agreement number 764066..

G. Alessandri and F. Gallorini work at VGA S.r.l., Via Foscolo, 1, 06053 Deruta (PG), Italy (email: giacomo.alessandri@vgasrl.com).

L. Castellini works at UMBRAGROUP S.p.A, Via V. Baldaccini, 1, 06034 Foligno (PG), Italy (email: lcastellini@umbragroup.com).

D. Montoya and E. F. Alves work at Norwegian University of Science and Technology, O.S. Bragstadsplass 2E, 7491 Trondheim, Norway (email: elisabetta.tedeschi@ntnu.no).

E. Tedeschi works at Norwegian University of Science and Technology, O.S. Bragstadsplass 2E, 7491 Trondheim, Norway and at University of Trento, Via Sommarive 9, 38123 Povo (TN) (email: elisabetta.tedeschi@ntnu.no).

The Electro-Mechanical Generator (EMG) is a linear device for wave energy applications developed by UMBRAGROUP, a company leader in the production of ballscrews, bearings and electro-mechanical actuators for the aerospace, industrial and energy sectors. The two key subsystems of the EMG are:

- the ballscrew, a mechanical device able to convert linear, reciprocating motion into a rotary motion with a high efficiency, thanks to the reduced rolling friction between ball and screw threads;
- the Permanent Magnet Synchronous Machine (PMSM), an electrical system where permanent magnets are bonded to a rotating element (rotor), which induces a voltage on the stator windings according to the principle of electro-magnetic induction.

The coupling of these two technologies creates a machine able to convert an input force at a certain speed in output electrical power. This concept has demonstrated remarkable performance in wave energy applications as shown in [7] and [8]. Moreover, the reversibility of the ballscrew and PMSM machines allows also to use the same device in reversed conditions, i.e. as a linear actuator.

For estimating the EMG preliminary loading envelope, three different device concepts and three deployment sites have been coupled, considering as initial constraint the 250kW EMG peak power. Fully coupled models in WEC-Sim [9] were created to integrate the EMG with the WEC concepts in a complete simulation environment and to evaluate their performances [10]. The concept selected and used for the EMG design was the Oscillating Wave Surge Converter (OWSC), thanks to the ability of the kinematics to constrain the maximum stroke, independently of the different load cases taken into account. The PTO system resulted in a design with four parallel EMGs, aiming at equally sharing the load from the prime mover among these units (Fig. 1). The EMGs are connected to the device flap through and arm lever, while the PTO fixed body is hinged to the seabed.

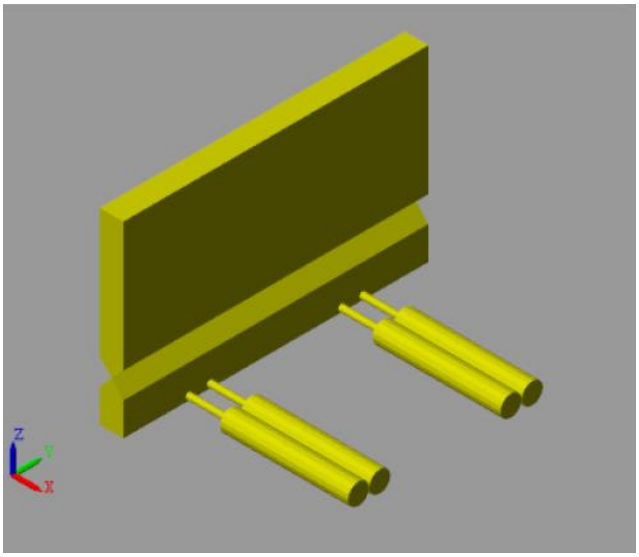

Fig. 1. WEC-Sim model for the OWSC concept with more EMGs in parallel configuration.

The consequences of parallelizing more EMG units have been also explored in [11]. As highlighted from the research, this practice can have benefits in reducing the peak forces at the PTO axis while maintaining a Mean Annual Energy Production similar to one sole, larger EMG unit.

Being the concept of parallelized EMG units one of the base hypotheses of the OWSC concept, UMBRAGROUP decided to approach the design of each EMG using two parallel Electro-Mechanical Units (EMUs) working in unison. This choice allows to demonstrate the modularity of the EMG, and the applicability of this principle to a higher number of parallelized units (as in the proposed OWSC model). Moreover, the use of two parallel units as an EMG provides significant advantages in terms of redundancy and reliability of the overall PTO system.

III. EMU DESIGN

Table I summarises the input data used by UMBRAGROUP for the design of a single EMU. These have been derived from the described OWSC model, assuming the power production load case. The management of eventual emergency conditions due to faults on the PTO system are closely related to WEC behaviour. Being this a topic outside of the IMAGINE project boundaries, the consequences of these load cases at a higher level have been neglected.

TABLE I
INPUT DATA FOR THE EMU DESIGN

Symbol	Quantity	Unit
*Prated**	44.4	kW
*Pmax**	125	kW
*Fmax***	82.5	kN
*Stroke***	4000	mm

*Values of the electrical machine.
**Values at the EMU input axis.

The first step in the EMU design process was the characterization of the concept architecture. This involved defining which of its core components, i.e. ballscrew and PMSM, would be fixed or moving. To achieve that, UMBRAGROUP carried out a weighted scoring process considering aspects such as reliability, maintainability, installation, heat dissipation, size, and mass. An architecture with moving ballnut and rotating screw has been chosen, as represented in Fig. 2.

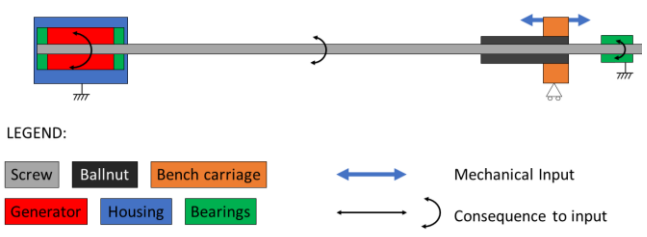

Fig. 2. Selected concept for the EMU architecture.

The following steps involved the detailed design of the EMU main components: ballscrew, electrical motor, bearings, flanges, housings, and choice of commercial components (Fig. 3). The EMU is equipped with a multi-turn absolute encoder at the rotor and thermal gauges embedded in the stator, which allows the PMSM to be controlled by the power converter. In addition, gauges measure the generator inner temperature for continuous monitoring during the device operation.

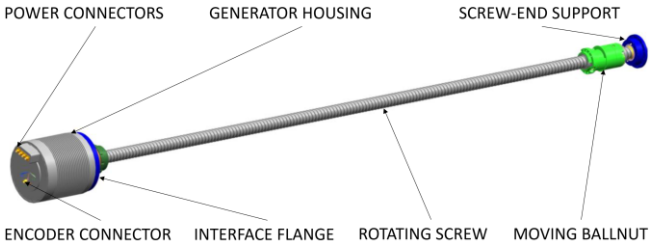

Fig. 3. EMU design.

IV. TEST RIG DESIGN

Following the definition of the EMU specifications, VGA initiated the test rig design by identifying the actuation system. This subsystem was prioritized due to its impact on the definition of other subsystems and on the overall budget. Both hydraulic and electro-mechanical actuators have been investigated to test the EMU according to its input design data (Table I).

Possible architectures for hydraulic cylinders included:

- a unidirectional system;
- a bidirectional system (actuation and generation);
- special cylinders with moving housings and a common high-pressure unit.

In general, two aspects were an obstacle to the effective exploitation of the hydraulic option: 1) the combination of high loads, long strokes and accelerations; 2) the high cost of a custom-made actuator and its power system.

As alternative, the application of high-power electrical actuators was evaluated and the possibility of exploiting the fully reversible EMU architecture was considered interesting. The use of two linear units in a parallelized arrangement, either as motors or generators, would give an additional confirmation of the device suitability for wave energy applications. This option, being technically viable and within the budget constraints, was chosen as the preferred one.

After that, the overall test setup was defined and divided into three main functional blocks: test rig, power management system, control software. Fig. 4 presents a functional block diagram that maps the main interfaces between components, including the power, signals and control flows.

The test rig structure (in black) features the integration of three EMUs with two of them mounted in parallel and connected to the third one by means of a carriage. This configuration allows: 1) using the EMU as an actuator to test the EMG; or 2) using the EMG as an actuator to test the EMU. The former test would be used to confirm the capability of EMUs to work in parallel, thus confirming the possibility to increase power and force of a generic PTO system by increasing the number of EMUs installed. The latter test would be used to confirm the adherence of the EMU to its design data.

The power management subsystem (in red) includes the power converters used to control the PMSMs, connected to a common DC bus and a Supply Unit interfaced with the grid. This electrical configuration allows the power from the device working as generator (either EMG or EMU) to be used by the actuating device. This results in the reduction of the Supply Unit power, accounting only for the inefficiencies of the overall system.

The control system (in olive) includes the WEC-Sim model used to simulate the kinematics of the OWSC during HIL tests. A Supervisory Control And Data Acquisition (SCADA) software interfaces simulation outputs and feedback from transducers mounted on the rig and the power converters.

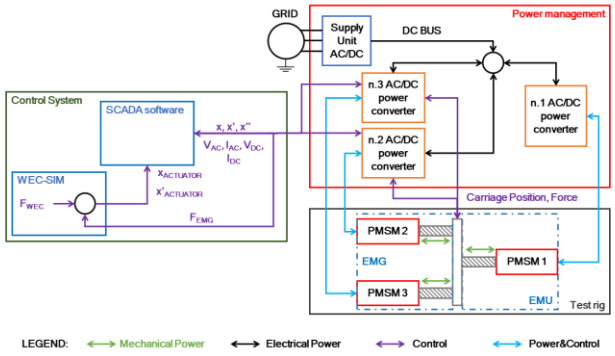

Fig. 4. HIL test rig functional block diagram.

Before sending the reference position to the actuator power converter, the SCADA software checks parameters of primary importance for the correct rig operation, comparing them to allowed limits set at the start-up phase. The parameters include: maximum instantaneous force, stroke, axial speed, EMU temperature, voltages, and currents. The estimation of load distribution between the main structural components is critical for the design of the test rig. A dynamic model of the rig mechanical structure was developed in Matlab Simulink to simulate its different operating conditions. The use of a multibody approach helped to confirm the EMG architecture choice and to identify the most severe conditions for the electrical subsystem. The components' mechanical properties (i.e. mass and size), disposition and constraints have been tuned according to a preliminary rig design. The Simulink model allowed to easily calculate the loads exchanged without the need of re-running time-consuming analyses. Fig. 5 shows the test rig model with the following parts displayed as simple geometric solids: support structure, anti-vibration feet, carriage, fixed flanges, ballscrews, housings and rotors.

To check and validate the model, simple working conditions (e.g. sinusoidal force profile) were simulated

and outputs were then compared to results calculated analytically by applying Newton's Second Law of Motion.

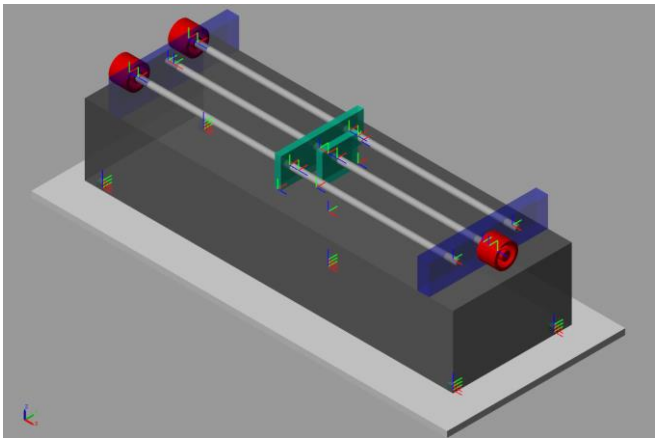

Fig. 5. HIL test rig Simulink model.

After this phase, operative and fault conditions were considered, according to the tests plan identified within the IMAGINE project [12]. Between these conditions, two main cases were considered of interest for the rig mechanical design: 1) the maximum operative load case; and 2) the maximum operative load case plus the occurrence of a fault. The first is associated with the values expressed in Table 1 and the second considers one of the PMSM or power converters subject to fault while the system is operating at maximum load. In this case, the other two PMSMs work as a brake to stop the carriage. Table II shows the overall test rig capabilities for operative tests, derived from the combination between design situations and characteristics of the actuation system.

TABLE II
TEST RIG CAPABILITIES FOR OPERATIVE TESTS

Symbol	Quantity	Unit
*Prated**	65	kW
*Pmax**	130	kW
*Fmax***	150	kN
*Stroke***	4240	mm

*Values at the motor's shaft.
**Values at the carriage.

V. DE-RISKING ANALYSIS

Once the test rig mechanical design and main electrical subsystems have been defined, NTNU carried out a de-risking analysis to evaluate and assess the effect of three-phase electrical faults on the rig during testing. After the definition of a WEC-Sim model with a detailed representation of the hydrodynamic, mechanical, control and electrical subsystems, two main configurations have been considered:

1) The EMG (namely PMSM 2 and 3 in Fig. 4) is generating while the EMU (PMSM 1 in Fig. 4) is actuating;
2) The EMG is actuating while the EMU is generating.

In the following paragraphs, the details of configuration 2 are described since this will be used to fully test the EMU, up to its maximum load. Fig. 6 represents the block diagram of the second configuration. The EMG axial position is supplied by the OWSC WEC-Sim model and fed into a position controller, directly connected to the actuator power converters (PMSM 2 and PMSM 3 drive). The position controller has the task of reproducing the WEC dynamics at the PTO input shaft. The drives set the voltage at the PMSMs inputs to actuate the rig carriage, connected to the ballnuts. For the EMU working as a generator (as indicated in Fig. 6), the carriage axial speed is used by the PTO controller to execute the selected control strategy and provide a torque reference to the generator power converter. In the context of the IMAGINE project, an adaptive PTO control strategy is applied to obtain the maximum power extraction for a given sea state.

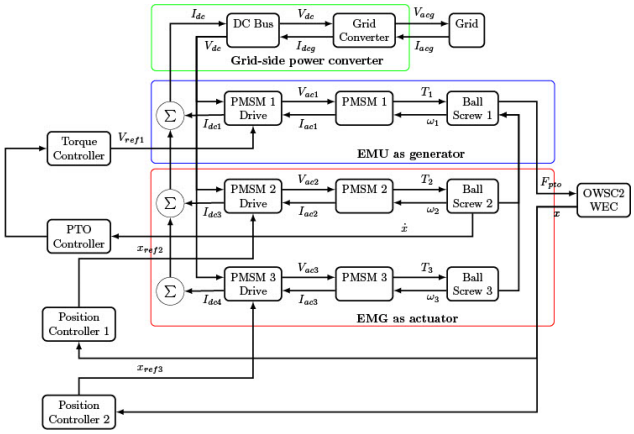

Fig. 6. Block diagram of the configuration 2.

The balance between input and output currents flowing throughout the three drives results in the DC bus current, to be supplied by the grid-side power converter from/to the grid. A safety control mode was implemented in the simulation to manage the fault after it is noticed. The fault is represented by a three phases resistance of 3 mΩ located between the PMSM and the power converter (Fig. 7). After the fault is detected, the switches from the generator side and the power converter side are tripped to clear the fault with a tripping delay time 100 ms.

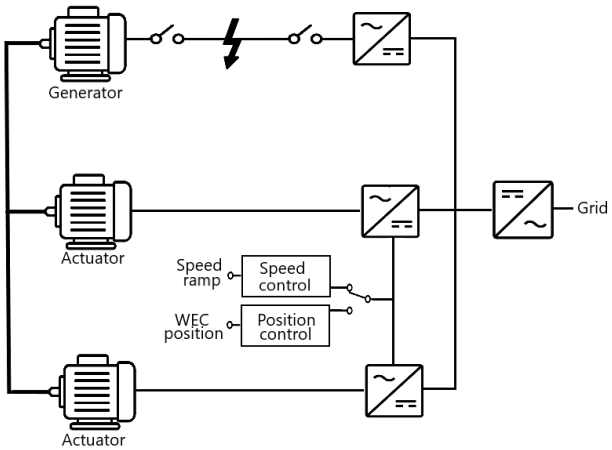

Fig. 7. Control scheme with a fault occurring between EMU (generator) and its power converter.

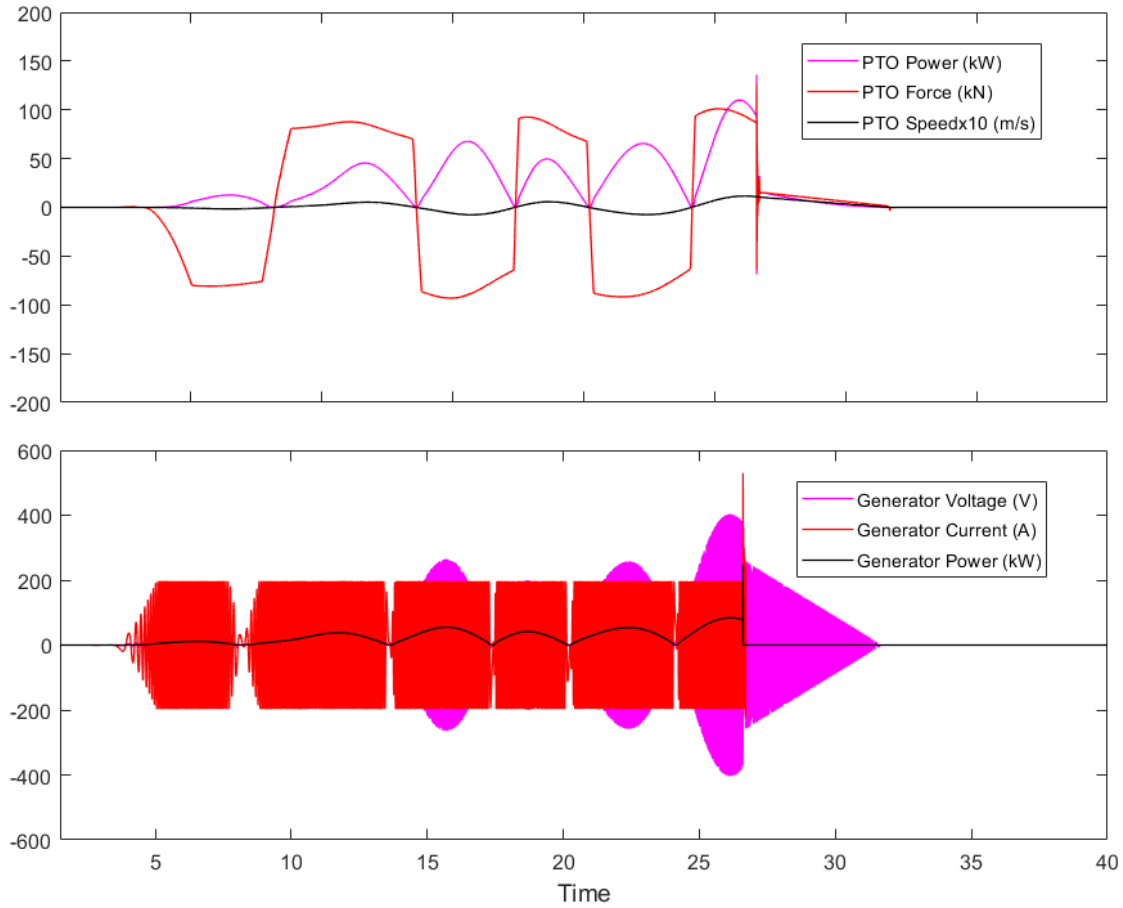

Fig. 8. Relevant mechanical (top) and electrical (bottom) signals of the generating EMU using configuration 2 when a fault occurs.

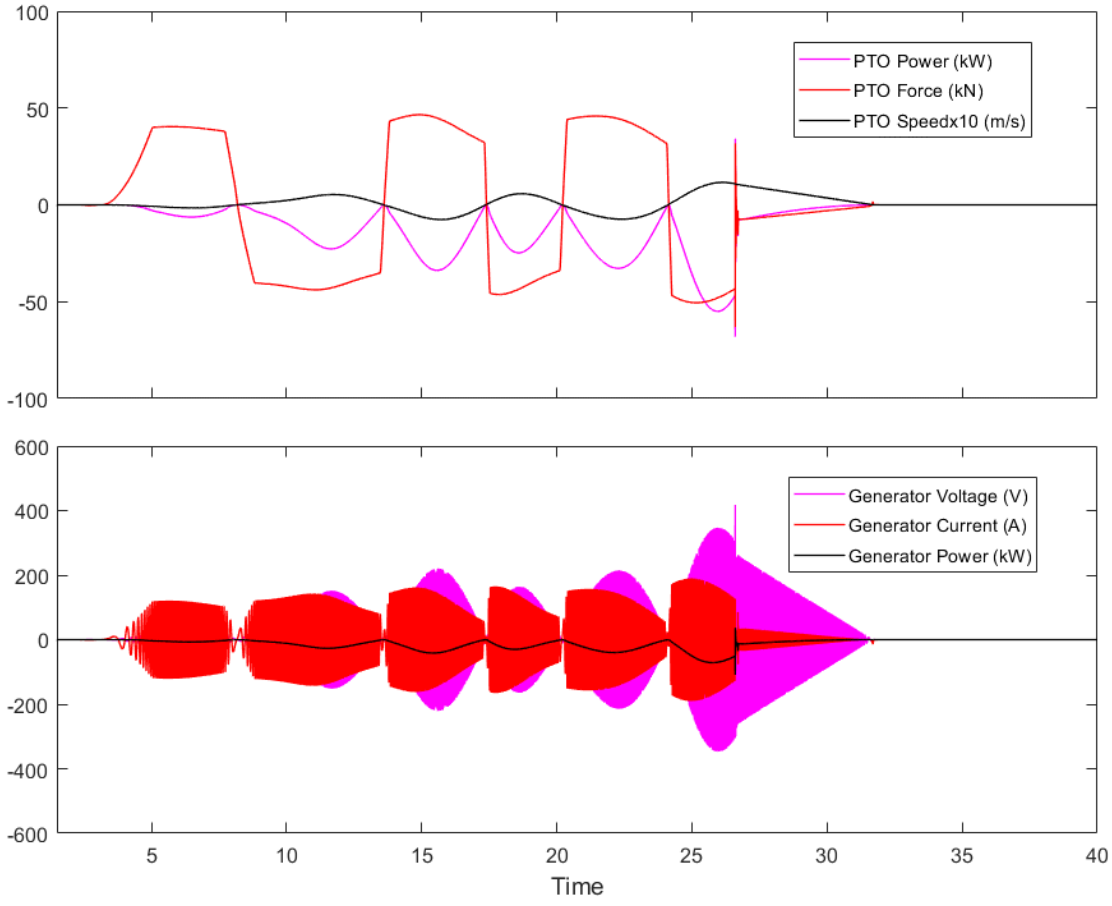

Fig. 9. Relevant mechanical (top) and electrical (bottom) signals of the actuating EMU using configuration 2 when a fault occurs.

After that timestep, the position control of the actuating EMGs is substituted by the safety speed control. The latter stops the system in a controlled manner, reducing the carriage axial speed from its current value to zero within a pre-defined time (set as 5 seconds in the simulation).

The fault was simulated by using one of the most energetic sea states previously defined for estimating the EMG loading environment. The simulation time was set in 40 s while the fault occurs at the time instant of 26.6 seconds. Fig.8 shows the simulation results for the main mechanical and electrical variables of the generating EMU. In normal operation, it is possible to notice the force profile at the PTO input axis, with a pseudo square-wave shape, related to the force-capped control used in the IMAGINE project.

The time instant related to the occurrence of the fault is noticeable from the power and force spikes: the maximum force in normal operating condition for the PTO is 82.5kN whereas it increases up to 126.27kN as a consequence of the high short circuit current.

At the same time, the mechanical power peaks due to the inertia of the PTO. It is also possible to see how the ramp speed profile is executed from the safety control mode. On the electrical side, peak currents of 529.75A (against a maximum value in normal operation of 197A) can be noticed, corresponding to a peak power of 249.74kW. Voltage signal shows a satisfactory behaviour after the fault since it correctly follows the set speed profile to stop the carriage.

TABLE III
SIMULATION RESULTS FOR GENERATOR - FAULT BETWEEN GENERATING UNIT AND ITS POWER CONVERTER

Symbol	Quantity	Unit
*Pmech,max**	136.12	kW
*Fmax**	126.27	kN
Pele,max	249.74	kW
Imax	529.75	A
Vmax	403.7	V

*Values at the PTO input axis.

Fig.9 shows the simulation results related to one of the two EMUs working as actuator, for the same parameters previously described. The mechanical signals are like the ones found for the generating EMU but halved in value thanks to the parallelized arrangement of the EMUs.

The electrical signals differ from the generating EMU in two aspects: the current does not present any peak while a voltage peak with a maximum value of 418.27V has been found just after the fault. The behaviour is associated to the switching manoeuvre between position and speed control and by the consequent balance between PTO and actuating forces. A maximum electrical power of 108.74kW has been measured, with oscillations before reaching the speed value set from the control strategy.

These oscillations also caused a negative value of electrical power, meaning the actuator converter is feeding power to the DC bus. Despite this, no remarkable effects are seen on the DC link and on the grid-side power converter, where the maximum voltage and current fall within the standard operating range.

TABLE IV
SIMULATION RESULTS FOR ACTUATOR - FAULT BETWEEN GENERATING UNIT AND ITS POWER CONVERTER

Symbol	Quantity	Unit
*Pmech,max**	68.06	kW
*Fmax**	63.13	kN
Pele,max	108.74	kW
Imax	190.33	A
Vmax	417.84	V

*Values at the PTO input axis.

Another simulated case consists in a fault occurring between one of the two actuators and the power converter. In this occurrence, both drives managing the EMUs working as actuators are disconnected and only the Generating Unit is applying force to stop the carriage, with a speed ramp different from the previous one. In either case (fault on actuating or generating unit), whenever the carriage would be positioned close to the end stroke of the test rig, the pre-defined ramp may require a distance longer than the available one. For this reason, the strokes of the EMUs and of the carriage have been separated into three parts:

1) The largest part (4000mm), where the PMSMs can slow down the carriage, by applying a torque opposed to its motion;
2) an extra-stroke (50mm per each side) that includes safety switches that are activated to disengage the PMSM and send an alarm to the SCADA software;
3) an emergency stroke (80 mm per each side) that hosts four end-stops, used to dissipate the remaining kinetic energy of the moving carriage.

Other conditions can be simulated by using the model described in this chapter; these may be useful to address specific test cases that are critical for a specific component.

VI. HARDWARE-IN-THE-LOOP SOFTWARE

The HIL software has been created starting from the WEC-Sim augmented model that NTNU produced in the de-risking analysis of the test rig. The main goals to achieve were two: 1) to verify the feasibility of running the augmented OWSC2 model in a real-time platform; 2) to integrate it with the higher lever controller of the rig (SCADA software).

The first task was assessed by NTNU in [13] by comparing the results of a real-time model to those of the de-risking process presented in section V.

The real-time model is divided into two subsystems. The *SC_GUI* subsystem integrates all the elements required for the supervision and control of the real-time simulation by the SCADA software. The *SM_PLANT* subsystem includes all the dynamic models required for

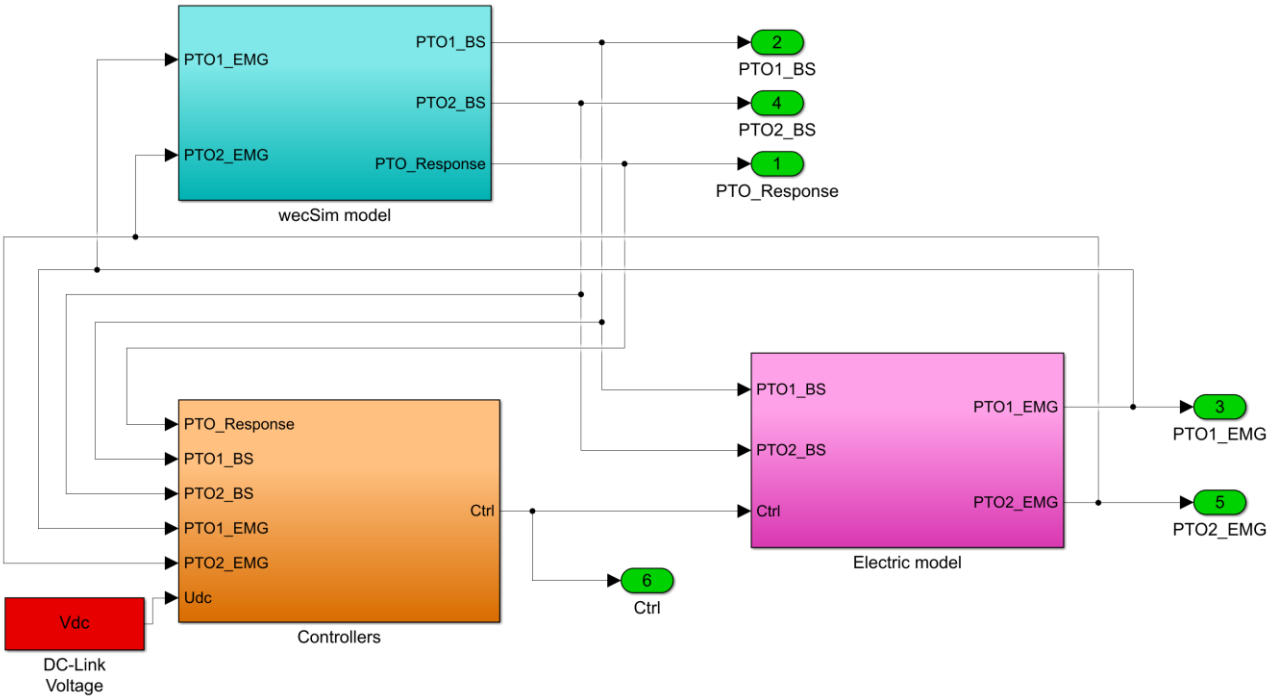

Fig. 10. Components of the SM_PLANT subsystem.

real-time simulation. Fig. 10 provides an overview of the blocks within this subsystem.

The *wecSim model* block integrates the OWSC model and the kinematics between the PMSMs and the WEC. This block receives the torque applied from the electrical generators in input and calculates the equilibrium between PTO system and hydrodynamic loads. The equilibrium defines the resulting position, speed, and acceleration at the EMG axis.

The *Controllers* block contains two different levels: a high-level controller that implements the proper PTO control strategy and defines the reference torque that the PMSM motor should apply to have a certain force at the input axis. A low-level controller defines the voltage to be applied at the PMSM input to achieve the reference torque.

The *Electric model* block comprises the proper model of the PMSM that, according to the input three-phase voltages and rotor speed, defines the output torque exerted at the PTO shaft and related currents.

The correspondence between the real-time model and the complete, augmented model used in the de-risking analysis was verified through the comparison of results for six different simulated conditions. The normalized root-mean-square error (NRMSE) was used as metric to quantitatively compare the two models:

$$\mathrm{NRMSE}\left(x_{RT}, x_{comp}\right) = 1 - \sqrt{\frac{\sum_{n=1}^{N}\left(x_{RT} - x_{comp}\right)^2}{\overline{x_{comp}}}} \qquad (1)$$

where N is the number of samples for the entire simulation and x_{RT}, x_{comp} are the values of the real-time and complete models respectively.

The results shown in Table V are related to the same conditions analyzed in fig. 8 and fig. 9. They reveal how the real-time model is capable of well replicating the PTO kinematics and power values. However, discrepancies on force, reference torque and output torque can be found.

TABLE V
COMPARISON BETWEEN COMPLETE AND REAL-TIME MODELS.

Symbol	NRMSE
Position *	0.986
*Velocity**	0.986
*Acceleration**	0.971
Force	0.870
Measured torque	0.855
Reference torque	0.842
*Mechanical power**	0.971
Electrical power	0.960

*Values at the PTO input axis.

These are due to the discretization of control loops in the real-time model and the different field weakening control strategy used in the two models. The former causes overshoot of the current controllers due to the additional delay introduced by the discretization of the PI controllers. To obtain the same response from the de-risking model, the current controllers in the real-time model have been re-tuned considering the delays introduced by discretization and by communication between the different parts of the system. The second source of discrepancy is due to the usage of a simplified, near-optimal solution of the field weakening technique, more suitable for embedded, real-time controls. This algorithm is a protective and preventive strategy to ensure that the technical voltage and current limits of the machine are respected [14].

In agreement with the specifications of the test rig, the HIL software was connected to a higher-level control system in charge of measuring the main parameters from the transducers and implementing checks on the maximum instantaneous values. The Human-Machine Interface of the SCADA software requires the rig operator to follow the transitions from one state to another to run a test, as represented in fig.11.

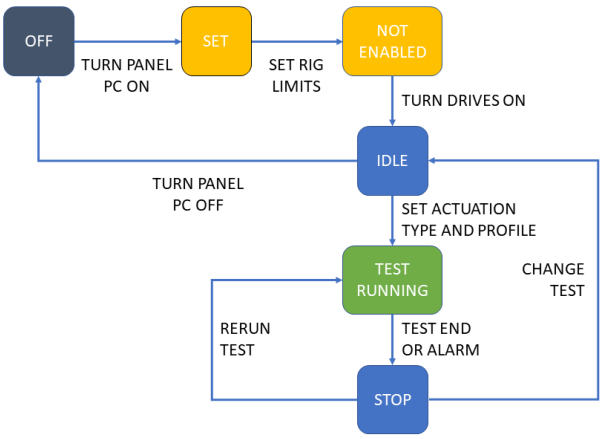

Fig. 11. States and transitions for the IMAGINE test rig software.

Once the control panel has been turned on, the limits of the test rig must be set. They include: the maximum force, maximum speed, maximum motor temperature and the stroke minimum and maximum values. After all the limits have been set, the power converters can be turned on and the settings of the actuation systems selected. These settings include the actuation type and profile. Actuation type is related to the parameter that the control system shall command during the test. Possible options are:

- carriage position;
- carriage speed;
- force at the carriage load cell.

The actuation profile can follow two pre-set profiles (trapezoidal or sinusoidal shaped), user-defined profiles (from time series uploaded to the control system) and real-time profiles (from the real-time HIL simulation).

Once these data have been input into the software, the test can be started. The test may be terminated in the following cases:

- the completion of the number of strokes set;
- the "stop" command from the rig user;
- the detection of an alarm.

An alarm is detected if the values measured from transducers during tests exceed the limits previously set. In this case, the SCADA software activates the alarm procedure and stops the test according to a pre-defined speed ramp profile.

The use of different actuation profiles is needed in the context of the IMAGINE project to check the alignment between the EMU model and the measured outputs. At the same time, the updated models can be used to re-run the de-risking simulation model, before starting the HIL testing phase. Moreover, initial tests can allow the rig user to understand practical aspects related to the behaviour of the hardware under test such as backlash between components and behaviour in transitions between static and dynamic conditions.

VII. TEST RIG MANUFACTURING

The final setup of the test rig mechanical assembly is represented in fig. 12. The rig structure is made up of a tubular frame, anti-vibration support feet and a top plate with threaded holes and slots. The EMUs are arranged to reduce the overall size of the rig: the central EMU housing is mounted on the left-side flange while the other two

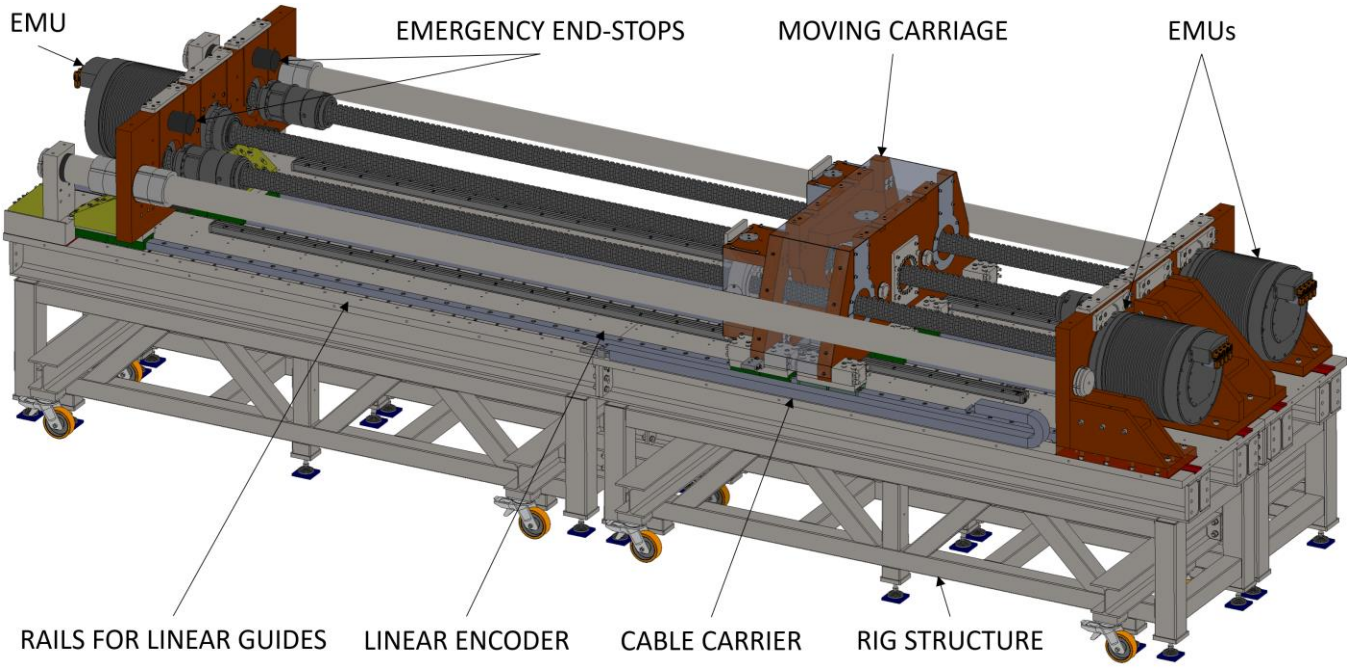

Fig. 12. HIL test rig mechanical assembly (3D view from CAD).

EMUs are mounted on the right-side flange. All the three ballnuts are connected to the same moving carriage, which integrates a load cell for measuring the force exchanged between the central EMU and the two on its sides. Four linear rails allow the motion of the carriage while three linear encoders measure the linear position of each EMU ballnut. The parallelized arrangement of the EMUs allowed to reach an overall rig structure of 6.5 m length and 2.1m width.

The design of the power management system was carried out by post-processing the loads corresponding to operative and fault conditions; particular attention was given to the latter, by finding out the cases of highest currents on power converters, DC bus and supply unit. The system is integrated in an electrical panel, divided into the following sections:

- PLC: it intregrates the Programmable Logic Controllers and other boards related to the processing of low-voltage, digital signals including safety aspects such as end-switches and emergency buttons. The signals are exchanged through an EtherCAT fieldbus, connected to the power converters and to the Control System.
- Auxiliary: it includes the 24V power supply and the interfaces for analog signals such as load cell and thermal gauges mounted on the EMUs' housings and other auxiliaries to the power converters and resistor (e.g. cooling fans). The analog signals are transformed into digital signals and sent to the PLC section.
- Incoming line: it includes the interface with the 690V_{AC} external line, safety fuses, ground bar and the power line to the Supply Unit.
- Supply Unit: it includes a bi-directional power converter which transforms the 690V_{AC} input voltage into the 1000V_{DC} that feeds the DC BUS.
- Drive EMU n.1, 2, 3: each of the three sections includes the power converters of the EMU, the interfaces with the PMSM thermal gauges, rotary encoder and linear encoder installed on the carriage. The measured values (rotary and linear positions, voltages, currents) are sent as digital data to the PLC section.
- Chopper: braking chopper to be activated in case of faults or whenever the power on the DC bus exceeds the limit defined by the Supply Unit.
- Braking resistor: group of grids and fans used to dissipate power, activated in cases of emergency.

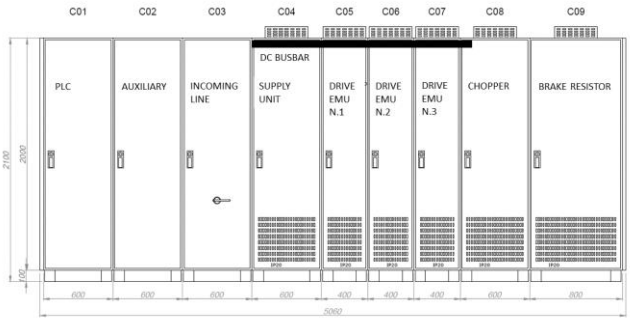

Fig. 13. Dimensional drawing of the electrical control panel.

The manufacturing phase of the test rig involved the welding of the tubulars to create the basement frame and the machining of all the other components mounted on the frame top surface.

The different manufacture phases were followed by acceptance tests; single components were tested by the respective suppliers while tests on main assemblies have been carried out by VGA. Tests involved dimensional, electrical and software checks. Acceptance tests have been undertaken to identify possible errors in the software or in the Human-Machine Interface.

Fig. 14. HIL test rig mechanical assembly.

The tests included the following checks:

- States and transitions;
- Replication of actuation profiles with only one EMU connected;
- Replication of alarms and emergency stop profiles.

VIII. Conclusions and Next Steps

A. Summary of key findings

This paper presented the main activities related to the modelling, design, de-risking, and manufacturing of a HIL test rig for linear PTOs. Following the PTO loading environment identified for the operative conditions, UMBRAGROUP designed an EMU with rotating ballscrew and moving ballnut.

The test rig has been designed by VGA, choosing to use EMUs as actuators, thanks to their fully bi-directional capability. A Simulink model of the test rig was developed to identify the most demanding conditions on its main structural components.

NTNU carried out an extensive de-risking activity by modelling the mechanical, electrical and control aspects, based on the design provided by UMBRAGROUP and VGA. Case studies with faults between electrical generator and power converter were analysed, leading to the identification of additional potential risks for the rig operation. Safety features including emergency end-stops and braking chopper were integrated in the rig structure and electrical panel respectively.

A HIL model of the overall rig was produced by NTNU, that pre-tested case studies to validate this model with the one previously used to de-risk the rig design.

VGA interfaced the HIL software with a higher-level controller, connected to the transducers mounted on the rig and on the electrical panel. The manufacturing phase involved the parallelized productions of the mechanical components, electrical parts, and software. Acceptance tests of the main mechanical sub-assemblies, of the overall control panel and of the control system have been conducted, to ensure adherence to design requirements.

B. Next steps

Next steps include the final commissioning phase involving the usage of the rig to test its main capabilities. The operation of the test rig, with the aim of executing the test plan identified in the context of the IMAGINE project, will include:

- characterization of the EMU static and dynamic losses;
- characterization of the EMU performances at constant speed conditions;
- characterization of the EMG performances;
- characterization of the EMU performances in HIL tests, with regular waves;
- characterization of the EMU performances in HIL tests, with irregular waves.

Finally, the results from the tests will be also used to update the EMG model, increasing further the fidelity of future analyses and tests.

Acknowledgement

The IMAGINE project has received funding from the European Union's Horizon 2020 research and innovation programme under grant agreement number 764066.

References

[1] Ocean Energy Forum, "Ocean Energy Strategic Roadmap 2016: Building ocean energy for Europe," Nov. 2016. [Online]. https://webgate.ec.europa.eu/maritimeforum/en/node/3962

[2] Carbon Trust, "Accelerating marine energy," Carbon Trust, UK, Tech. Rep. CTC797, Jul. 2011. [Online]. Available: https://prod-drupal-files.storage.googleapis.com/documents/resource/public/Accelerating%20marine%20energy%20-%20REPORT.pdf

[3] G. Bacelli, S. Spencer, R. Coe, A. Mazumdar, D. Patterson, K. Dullea, "Design and Bench Testing of a Model-Scale WEC for Advanced PTO Control Research" in Proc. of the *12th European Wave and Tidal Energy Conference*, 2017, Cork, Ireland.

[4] G. Bracco, E. Giorcelli, G. Mattiazzo, V. Orlando M. Raffero, "Hardware-in-the-loop test rig for the ISWEC wave energy system", *Mechatronics*, Vol. 25, pp. 11-17, 2015.

[5] H. Pedersen, R. Hansen, A. Hansen, T. Andersen, and M. Bech, "Design of full scale wave simulator for testing Power Take Off systems for wave energy converters," *International Journal of Marine Energy*, vol. 13, pp. 130–156, Apr. 2016.

[6] S. Armstrong, J. Rea, F.-X. Faÿ, E. Robles, "Lessons learned using electrical research test infrastructures to address the electrical challenges faced by ocean energy developers", *International Journal of Marine Energy*, Volume 12, pp. 46-62, 2015.

[7] L. Castellini, M. Martini and G. Alessandri, "Development and testing of a ballscrew Electro- Mechanical Generator (EMG) for wave energy conversion" in Proc. of *12th European Wave and Tidal Energy Conference*, 2017, Cork, Ireland.

[8] L. Castellini and G. Alessandri, "Dry and Wet Testing of a PTO Based on Recirculating Ballscrew Technology" in Proc. of *3rd Asian Wave and Tidal Energy conference*, 2016, Singapore.

[9] Y.-H. Yu, K. Ruehl, J. V. Rij, N. Tom, D. Forbush, D. Ogden, A. Keester, and J. Leon, "Wec-sim v4.2," Dec. 2020. [Online]. Available: DOI 10.5281/zenodo.3924764.

[10] J. Cruz, M. Actheson, J. Scriven, T. Martins, L. Castellini and M. Martini, "Preliminary Load Assessment: UMBRA's 250kW EMG Power Take-Off" in Proc. of the *13th European Wave and Tidal Energy Conference*, 2019, Naples, Italy.

[11] J. Scriven, J. Cruz and M. Actheson, "Upscaling Wave Energy Converters: Size vs. Modularity" in Proc. of the *4th International Conference on Renewable Energies Offshore*, 2020, Lisbon, Portugal.

[12] IMAGINE project. (2019). D6.1 – EMG test procedure report (Issue 01, dated 11/03/2019).

[13] L. Castellini, E. Alves, D. Montoya, F. Gallorini, G. Alessandri, E. Tedeschi, "Performance Comparison of Offline and Real-Time Models of a Power Take-Off for Qualification Activities of Wave Energy Converters", in Proc. of the *16th International Conference on Ecological Vehicles*, 2021 (accepted for publication).

[14] S. Lim, "Sensorless-FOC With Flux-Weakening and MTPA for IPMSM Motor Drives," Texas Instruments, Tech. Rep. SPRACF3, 2018. [Online]. Available: https://www.ti.com/lit/an/spracf3/spracf3.pdf